別添４

研究成果の刊行に関する一覧表

書籍

著者氏名	論文タイトル名	書籍全体の編集者名	書　籍　名	出版社名	出版地	出版年	ページ
該当なし。							

雑誌

発表者氏名	論文タイトル名	発表誌名	巻号	ページ	出版年
Hayashi, H., Shimamoto, K., Taniai, E., Ishii, Y., Morita, R., Suzuki, K., Shibutani, M., Mitsumori, K.	Liver tumor promoting effect of omeprazole in rats and its possible mechanism of action.	J Toxicol Sci	37(3)	491-501	2012
Hayashi, H., Taniai, E., Morita, R., Yafune, A., Suzuki, K., Shibutani, M., Mitsumori, K.	Threshold dose of liver tumor promoting effect of β-naphthoflavone in rats.	J Toxicol Sci	37(3)	517-526	2012
Hayashi, H., Taniai, E., Morita, R., Hayashi, M., Nakamura, D., Wakita, A.,Suzuki, K., Shibutani, M.,Mitsumori, K.	Enhanced liver tumor promotion but not liver initiation activity in rats subjected to combined administration of omeprazole and β-naphthoflavone.	J Toxicol Sci	37(5)	969-985	2012
Yafune, A., Taniai, E., Morita, R., Nakane, F., Suzuki, K., Mitsumori, K., Shibutani, M.	Expression patterns of cell cycle proteins in the livers of rats treated with hepatocarcinogens for 28 days.	Arch Toxicol	in press		2013
Yafune, A., Taniai, E., Morita, R., Hayashi, H.,Suzuki, K., Mitsumori, K., Shibutani, M.	Aberrant activation of M phase proteins by cell proliferation-evoking carcinogens after 28-day administration in rats.	Toxicol Lett	219(3)	203-210	2013
Morita, R., Yafune, A., Shiraki, A., Itahashi, M., Ishii, Y., Akane, H., Nakane, F., Suzuki, K., Shibutani, M., Mitsumori, K.	Liver tumor promoting effect of orphenadrine in rats and its possible mechanism of action including CAR activation and oxidative stress.	J Toxicol Sci	38(3)	403-413	2013
Morita, R., Yafune, A., Shiraki, A., Itahashi, M., Akane, H., Nakane, F., Suzuki, K., Shibutani, M., Mitsumori, K.	Enhanced liver tumor promotion activity in rats subjected to combined administration of phenobarbital and orphenadrine.	J Toxicol Sci	38(3)	415-424	2013

研究成果の刊行物・別刷

Arch Toxicol
DOI 10.1007/s00204-013-1011-y

GENOTOXICITY AND CARCINOGENICITY

Expression patterns of cell cycle proteins in the livers of rats treated with hepatocarcinogens for 28 days

Atsunori Yafune · Eriko Taniai · Reiko Morita · Fumiyuki Nakane · Kazuhiko Suzuki · Kunitoshi Mitsumori · Makoto Shibutani

Received: 23 September 2012 / Accepted: 17 January 2013

Abstract Some hepatocarcinogens induce cytomegaly, which reflects aberrant cell cycling and increased ploidy, from the early stages of administration to animals. To clarify the regulatory molecular mechanisms behind cell cycle aberrations related to the early stages of hepatocarcinogenesis, we performed gene expression analysis using microarrays and real-time reverse transcription polymerase chain reaction followed by immunohistochemical analysis in the livers of rats treated with the cytomegaly inducing hepatocarcinogens thioacetamide (TAA), fenbendazole, and methyleugenol, the cytomegaly non-inducing hepatocarcinogen piperonyl butoxide (PBO), or the non-carcinogenic hepatotoxicants acetaminophen and α-naphthyl isothiocyanate, for 28 days. Gene expression profiling showed that cell cycle-related genes, especially those of G_2/M phase, were mostly upregulated after TAA treatment. Immunohistochemical analysis was performed on cell cycle proteins that were upregulated by TAA treatment and on related proteins. All hepatocarcinogens, irrespective of their cytomegaly inducing potential, increased liver cells immunoreactive for $p21^{Cip1}$, which acts on cells arrested in G_1 phase, and for Aurora B or Incenp, which is suggestive of an increase in a cell population with chromosomal instability caused by overexpression. PBO did not induce cell proliferation after 28-day treatment. Hepatocarcinogens that induced cell proliferation after 28-day treatment also caused an increase in $p53^+$ cells in parallel with increased apoptotic cells, as well as increased population of cells expressing M phase-related proteins nuclear Cdc2, phospho-Histone H3, and HP1α. These results suggest that hepatocarcinogens may increase cellular populations arrested in G_1 phase or showing chromosomal instability after 28-day treatment. Hepatocarcinogens that induce cell cycle facilitation may cause M phase arrest accompanied by apoptosis.

Keywords Hepatocarcinogen · Cell cycle · Cytomegaly · Prediction marker

Abbreviations

ANIT	α-Naphthyl isothiocyanate
APAP	Acetaminophen
Cdc2	Cell division cycle 2
Cdk	Cyclin-dependent kinase
FB	Fenbendazole
HP1α	Heterochromatin protein 1α
Klf6	Kruppel-like factor 6
MEG	Methyleugenol
NDRG1	N-myc downstream regulated gene 1
p-Histone H3	Phosphorylated-Histone H3
PBO	Piperonyl butoxide
TAA	Thioacetamide
Topo IIα	Topoisomerase IIα

Electronic supplementary material The online version of this article (doi:10.1007/s00204-013-1011-y) contains supplementary material, which is available to authorized users.

A. Yafune · E. Taniai · R. Morita · F. Nakane · K. Suzuki · K. Mitsumori · M. Shibutani (✉)
Laboratory of Veterinary Pathology, Tokyo University of Agriculture and Technology, 3-5-8 Saiwai-cho, Fuchu-shi, Tokyo 183-8509, Japan
e-mail: mshibuta@cc.tuat.ac.jp

A. Yafune · E. Taniai · R. Morita
Pathogenetic Veterinary Science, United Graduate School of Veterinary Sciences, Gifu University, 1-1 Yanagido, Gifu-shi, Gifu 501-1193, Japan

A. Yafune
Gotemba Laboratory, Bozo Research Center Inc., 1284 Kamado, Gotemba, Shizuoka 412-0039, Japan

Published online: 15 February 2013

Introduction

The currently used methods for the evaluation of the carcinogenicity of chemicals are bioassays in which rodents are treated with the chemical for their entire 1.5- or 2-year life span. Long-term carcinogenicity studies using experimental animals are time-consuming, expensive, and involve the use of many animals. Medium-term carcinogenesis bioassays using rat liver or multi-organ models (Tamano 2010) or genetically modified animals using transgenic or gene targeting technologies (Eastin 1998) are used as alternative models. However, they are also expensive and time-consuming and often have limited target organs. Toxicogenomic approaches for prediction of carcinogenic potential in each target organ appear promising. Unfortunately, these are also expensive and require integrative methodologies between different laboratories sharing an expression database (Uehara et al. 2011). There is no commonly used rapid means of evaluating the carcinogenic potential of chemicals that can be used for genotoxic and non-genotoxic carcinogens. Therefore, it is essential to establish a short-term carcinogenicity screening system based on the molecular responses to the carcinogens in the target organs.

Evaluation of carcinogenicity study data collected in the National Toxicology Program (NTP) showed that prechronic liver lesions including hepatocellular necrosis, hepatocellular hypertrophy, hepatocellular cytomegaly, bile duct hyperplasia, and hepatocellular degeneration, along with increased liver weight in the prechronic studies may be used as components in the search for predictors of liver carcinogenicity in chronic 2-year bioassays (Allen et al. 2004). Some hepatocarcinogens induce cytomegaly characterized by the presence of hepatocytes with increased cytoplasmic volume and karyomegaly from the early stages of exposure (Allen et al. 2004; Hamadeh et al. 2004). The development of cytomegaly is suggestive of cell cycle aberrations causing chromosomal instability through nuclear division during mitosis. Mitotic aberrations such as chromosomal missegregation and cytokinesis failure occurring as a result of checkpoint dysfunction of the cell cycle can result in tetraploidy/aneuploidy (Ichijima et al. 2010).

Recent studies have shown that ochratoxin A, a renal carcinogen, can induce karyomegaly with DNA aneuploidy and polyploidy accompanied by abnormal expression of cell cycle proteins, especially G_2/M phase-related proteins (Adler et al. 2009). These cellular events may lead to chromosomal instability. Moreover, development of karyomegaly is also observed during carcinogenesis in the kidney and large intestine (Williams et al. 2002; Adler et al. 2009), suggesting a common mechanism for carcinogenesis across target organs. Therefore, we hypothesize that there is an early event in the carcinogenic response that causes the development of karyomegaly/cytomegaly by disrupting cell cycle regulation. We have previously analyzed cell cycle proteins in a study of 28-day repeated treatment with renal carcinogens to induce karyomegaly in rats (Taniai et al. 2012). We found that renal carcinogens, irrespective of karyomegaly inducing potential, increased the number of proximal tubular cells positive for Ki-67, a cell proliferation marker, and topoisomerase IIα (Topo IIα), suggesting that proliferation is accompanied by cell cycle aberration. These findings suggest that carcinogens may activate target cell proliferation after short-term repeated exposure.

In the present study, to further examine the regulatory molecular mechanisms behind cell cycle aberrations during the early stages of hepatocarcinogenesis, we first carried out global gene screening using microarrays in the liver of rats receiving repeated oral administration of thioacetamide (TAA), a representative cytomegaly inducing hepatocarcinogen, and then real-time reverse transcription polymerase chain reaction (RT-PCR) analysis in the livers of rats receiving TAA or fenbendazole (FB). We selected cell cycle-related genes based on the gene expression data. Localization of candidate proteins showing upregulation of mRNA and related proteins were further analyzed immunohistochemically in the livers of rats receiving the cytomegaly inducing hepatocarcinogens TAA, FB, and methyleugenol (MEG), the cytomegaly non-inducing hepatocarcinogen piperonyl butoxide (PBO), or the non-carcinogenic hepatotoxicants acetaminophen (APAP) and α-naphthyl isothiocyanate (ANIT) for 28 days.

Materials and methods

Chemicals

Thioacetamide (TAA; CAS No. 62-55-5, ≥98.0 %) and sterilized 0.5 % (w/v) methyl cellulose 400 solutions were purchased from Wako Pure Chemicals Industries (Osaka, Japan). Methyleugenol (MEG; CAS No. 93-15-2, >98.0 %), acetaminophen (APAP; CAS No. 103-90-2, ≥98.0 %), and α-naphthyl isothiocyanate (ANIT; CAS No. 551-06-4, ≥98.0 %) were purchased from Tokyo Chemical Industry Co. (Tokyo, Japan). Fenbendazole (FB; CAS No. 43210-67-9, ≥98.0 %) was purchased from LKT Laboratories, Inc (St. Paul, MN, USA), and piperonyl butoxide (PBO; CAS No. 51-03-6, ≥98.0 %) from Nagase & Co. (Osaka, Japan).

Animal experiments

Animals and experimental design were identical to those previously reported (Taniai et al. 2012). Animal studies were conducted in accordance with the institute Guide for Animal Experimentation, given free access to powdered

diets, and were maintained under standard conditions (room temperature, 23 ± 3 °C; relative humidity, 50 ± 20 %, 12-hour light/dark cycle). Briefly, 5-week-old male F344/NSIc rats (Japan SLC, Inc., Hamamatsu, Japan) were acclimatized to a powdered basal diet (Oriental Yeast Co., Tokyo, Japan) and tap water ad libitum for 1 week. Animals were randomized into groups of 10 animals and treated with TAA (400 ppm in the diet), FB (3,600 ppm in the diet), PBO (20,000 ppm in the diet), MEG (1,000 mg/kg body weight, daily by gavage), APAP (12,500 ppm in the diet), or ANIT. For ANIT, the initial dose was set at 1,000 ppm in the diet. However, as the general condition of the animals worsened, the dose was gradually reduced to 800 ppm for 14 days and 600 ppm for the following 7 days. TAA, FB, PBO, and MEG were selected as hepatocarcinogens/promoters in rats, and the dose levels of these compounds have shown to induce liver tumors or promote liver carcinogenesis in rats (Becker 1983; Takahashi et al. 1994; Shoda et al. 1999; NTP 2000; Ichimura et al. 2010). APAP and ANIT were selected as non-carcinogenic hepatotoxicants, and the dose of these compounds has shown to induce hepatotoxicity after 13- or 16-week administration in rats (Rees et al. 1962; NTP 1993). Ten untreated control animals were maintained on the basal diet and tap water without any treatment during the experimental period. One day after the 28-day treatment period, all animals were killed by exsanguination from the abdominal aorta under deep anesthesia and livers were removed.

Expression microarray analysis

Total RNA was extracted with the RNeasy Mini Kit (Qiagen, Hilden, Germany) according to the manufacturer's instructions. Using 10 μg of total RNA from one animal in the TAA-treatment group and one untreated control, double-stranded cDNA was synthesized with the Invitrogen Superscript Double-Stranded cDNA Synthesis Kit (Invitrogen Corp., Carlsbad, CA, USA), according to the manufacturer's protocol. The cDNA sample was labeled with Cy3 and loaded onto the *Rattus norvegicus* Roche NimbleGen microarray (Roche NimbleGen: Euk Expr 4x72k Catalog Arr, 26,208 targets; Roche Applied Science, Penzberg, Germany). Using the robust multiple average normalization method (Irizarry et al. 2003), differentially expressed genes were analyzed. Gene information was retrieved from the National Center for Biotechnology Information website (http://www.ncbi.nlm.nih.gov).

Real-time RT-PCR analysis

For confirmation of the microarray data, fluctuating transcript levels of representative cell cycle-related genes were subjected to mRNA expression analysis using the StepOnePlus™ Real-time RT-PCR System (Applied Biosystems Japan Ltd., Tokyo, Japan) with the SYBR® Green PCR Master Mix (Applied Biosystems Japan Ltd.). The forward and reverse primers listed in Table 1 were designed using the Primer Express 3.0 software (Applied Biosystems Japan Ltd.). Using the threshold cycle values of β-actin in the same sample as the endogenous control, the relative differences in gene expression were calculated using the $2^{-\Delta\Delta C_T}$ method (Livak and Schmittgen 2001).

Immunohistochemistry

Immunohistochemistry of liver sections was performed using the horseradish peroxidase avidin–biotin complex method using a VECTASTAIN® Elite ABC Kit (Vector Laboratories Inc., Burlingame, CA, USA), with the antibodies listed in Table 2 and 3,3'-diaminobenzidine/H_2O_2 as the chromogen. Antigen retrieval conditions for each antibody are shown in Table 2. Sections were counterstained with hematoxylin for microscopic examination.

Apoptosis assay

Liver sections were subjected to terminal deoxynucleotidyl transferase-mediated dUTP nick-end labeling (TUNEL) assay using the ApopTag® Peroxidase *In Situ* Apoptosis Detection Kit (Millipore, Billerica, MA, USA) according to the manufacturer's protocol. Briefly, deparaffinized sections were treated with 20 μg/ml proteinase K for 15 min at room temperature. Endogenous peroxidase activity was blocked with 3.0 % hydrogen peroxide. Color development and counter staining were as described in the immunohistochemistry section above.

Analysis of immunoreactivity

The immunostained cells were counted in 10 randomly selected areas per animal, avoiding portions of connective tissues and vasculature at a magnification of 200×. Immunoreactive liver cells were counted visually, and the total number of liver cells in the micrographs was separately counted using the image binarization method in the WinROOF image analysis and measurement software (version 6.4.2., Mitani Corporation, Fukui, Japan). The percentage of total immunoreactive cells in the 10 areas was estimated in each animal. A two-step screening system was applied for the analysis of antigen immunoreactivity in terms of cellular distribution in relation to carcinogen treatment. For first screening of proteins, livers from 5 animals per group were subjected to analysis. If a significant difference in the distribution of positive cells was observed between the untreated controls or non-carcinogens and carcinogens, the remaining 5 animals were similarly subjected to analysis for the second screening.

Table 1 Sequence of primers used for real-time RT-PCR analysis

Accession no.	Symbol	Forward primer[a]	Reverse primer
NM_130812	*Cdkn2b*	CCCTCACCAGACCTGTGCAT	CAGGCGTCACACACATCCA
NM_080782	*Cdkn1a*	ACCAGCCACAGGCACCAT	CGGCATACTTTGCTCCTGTGT
NM_171992	*Ccnd1*	GCGAGCCATGCTTAAGACTGA	CCCTCTGCACGCACTTGA
NM_053702	*Ccna2*	TGTCTCTGGTGGGTTGAGAAGA	ACCACAGCATGCCCAACAG
XM_001064075	*Ccne2*	TCTCCACAAGAAGCCCAGATAATT	GGTGATCTCCTCTGTTCTTTTTTTG
NM_001025682	*Cdr2*	CAAGGCCTCACAGCAGAAAATC	GAGGTGATCAATGTTGGTTTGC
NM_001012742	*Wee1*	CGGCAAACTCCTCAAGTGAATATT	CACTGTCCTGAGGAATGAAGCAT
NM_001107790	*Tpx2*	CCCAAGAGACCACCTGTTAAGC	ACTCTCGCTCATGAATTCGTTTCT
NM_024127	*Gadd45a*	CACCATAACTGTCGGCGTGTA	GGCACAGGACCACGTTGTC
NM_019296	*Cdk1*	GGTCGCCAGAGGTGTTGCT	TCTGCAAATATGGTCCCTATGCT
NM_171991	*Ccnb1*	TGTCCCACACGGAAGAATCTCT	GGCCACGGTTCACCATGA
NM_053749	*Aurkb*	CGGATGCATAATGAGATGGTAGAT	TCCCCACCATCAGTTCATAGC
NM_153296	*Aurka*	AAGAGAGTCATCCACAGAGACATCAA	CGATCTTCAACTCCCCATTTG
NM_030989	*Tp53*	CATGAGCGTTGCTCTGATGGT	GATTTCCTTCCACCCGGATAA
NM_001108099	*Mdm2*	GAAGGAGGACACACAAGACAAAGA	ATGGCTCGATGGCGTTCA
NM_001011991	*Ndrg1*	GTCACACCTTGTCTCCCATTATTG	CCAGGTGAGAGACATTCAGTTATCA
NM_031642	*Klf6*	GCGCCATCCAGTTTGCAT	GATCAGGAGTCGGAGCAGAAA
NM_031144	*Actb*	CCCTGGCTCCTAGCACCAT	AGAGCCACCAATCCACACAGA

Aurk aurora kinase, *Actb* actin beta, *Ccn* cyclin, *Cdk* cyclin-dependent kinase, *Cdkn* cyclin-dependent kinase inhibitor, *Cdr2* cerebellar degeneration-related 2, *Gadd45a* growth arrest and DNA-damage-inducible, alpha, *Klf6* Kruppel-like factor 6, *Mdm2* p53 binding protein homolog (mouse), *Ndrg1* N-myc downstream regulated 1, *RT-PCR* reverse transcription polymerase chain reaction, *Tp53* tumor protein p53, *Tpx2* microtubule-associated, homolog (*Xenopus laevis*), *Wee1* wee 1 homolog (*S. pombe*)

[a] The primer sets were designed using the Primer Express® software (Version 3.0; Applied Biosystems Japan Ltd.)

Table 2 Antibodies used in the present study

Antigen	Host species	Clonality	Dilution	Antigen retrieval[a]	Manufacturer (city, state, country)
Ki-67	Mouse	Monoclonal	1:50	Autoclaving	Dako (Glostrup, Denmark)
Cdc2 p34	Mouse	Monoclonal	1:100	None	Santa Cruz Biotechnology, Inc. (Dallas, TX, USA)
Histone H3 (Ser 10 phosphorylated)	Rabbit	Polyclonal	1:50	Autoclaving	Santa Cruz Biotechnology, Inc.
HP1α	Rabbit	Polyclonal	1:200	Microwaving	Cell Signaling Technology, Inc. (Danvers, MA, USA)
Aurora B	Rabbit	Polyclonal	1:200	None	Abcam (Cambridge, UK)
Incenp	Rabbit	Polyclonal	1:500	Autoclaving	Abcam
p53	Rabbit	Polyclonal	1:100	Autoclaving	Santa Cruz Biotechnology, Inc.
$p21^{Cip1}$	Mouse	Monoclonal	1:100	Microwaving	Abcam
$p27^{Kip1}$	Rabbit	Polyclonal	1:100	None	Cell Signaling Technology, Inc.
$p16^{Ink4a}$	Mouse	Monoclonal	1:100	None	Santa Cruz Biotechnology, Inc.
Wee1 (Ser 53 phosphorylated)	Rabbit	Polyclonal	1:100	Microwaving	Assay Biotechnology Co. Inc. (Sunnyvale, CA, USA)

[a] Antigen retrieval was applied to immunohistochemistry. Retrieval conditions were either autoclaving at 121 °C for 10 min or by microwaving at 90 °C for 10 min in 10 mM citrate buffer (pH 6.0)

Statistical analysis

Numerical data are represented as mean ± SD. All data were analyzed by the Bartlett's test for the homogeneity of variance. If there was no significant difference in variance, Dunnett's test was performed for comparison between the groups. If a significant difference was found in variance, Steel's test was performed. With regard to final body and

Table 3 Final body and liver weights of rats after 28-day treatment with hepatocarcinogens or hepatotoxicants

Group	No. of animals examined	Final body weight (g)	Liver weight	
			Absolute (g)	Relative (g/100 g BW)
Untreated controls	10	210±16[a]	7.93±0.87	3.68±0.17
TAA	10	141±13**	7.08±0.87*	4.94±0.24**
FB	10	208±14	8.62±0.68	4.04±0.14**
PBO	10	164±10**	11.89±0.77**	7.16±0.18**
MEG	10	175±13**	10.09±0.89**	5.68±0.31**
APAP	10	173±9**	7.17±0.55*	4.07±0.15**
ANIT	10	111±5**	6.43±0.44**	5.70±0.21**

* $P < 0.05$ versus untreated controls

** $P < 0.01$ versus untreated controls

[a] Mean ± SD

liver weights and real-time RT-PCR analyses, numerical data of the treatment groups were compared with those of the untreated controls. In case of the immunohistochemical analyses, numerical data were compared among all treatment groups and the untreated controls. Comparison between the APAP or ANIT and other treatment groups was similarly performed, excluding the untreated controls from comparison.

Results

Final body and liver weights

The final body and liver weights are shown in Table 3. As compared with the untreated controls, final body weights were significantly decreased in the TAA, PBO, MEG, APAP, and ANIT groups. The absolute liver weights of rats in the TAA, APAP, and ANIT groups were significantly lower than those of the untreated controls. The absolute liver weights of rats in the PBO and MEG groups were significantly higher than those of the untreated controls, but those of the FB group were not significantly changed. The relative liver weights of all treatment groups were significantly higher than those of the untreated controls.

Histopathological changes

Treatment with TAA induced diffuse liver cell cytomegaly often associated with anisokaryosis, aberrant mitosis, and apoptosis, as previously reported (Clawson et al. 1992). Bile duct proliferation and oval cell proliferation accompanied with mild interstitial fibrosis were evident in the periportal area. FB treatment induced centrilobular liver cell hypertrophy characterized by a marked increase in smooth endoplasmic reticulum, as previously reported (Shoda et al. 1999). Periportal liver cells showed cytomegaly associated with anisokaryosis and scattered mitoses. PBO treatment induced diffuse liver cell hypertrophy associated with cytoplasmic ground appearance and moderate nuclear enlargement, as previously reported (Muguruma et al. 2007). MEG treatment resulted in diffuse distribution of cytomegalic liver cells associated with anisokaryosis, as previously reported (NTP 2000). Centrilobular liver cell necrosis was also scattered. APAP treatment resulted in cytoplasmic eosinophilia and ground glass appearance of liver cells and ANIT treatment resulted in periportal bile duct proliferation, and scattered focal liver cell necrosis and microgranulomas, as previously reported (NTP 1993; Rees et al. 1962). However, neither APAP nor ANIT induced karyomegaly or cytomegaly in the liver cells.

Global gene expression changes after TAA treatment

Among the 26,208 gene targets identified in the microarray analysis, 2,888 genes showed altered expression in liver tissue after 28 days of TAA treatment compared to the untreated controls (1,681 genes were upregulated and 1,207 genes were downregulated, Online Resource 1). Most of the identified upregulated genes were related to cell proliferation, apoptosis, cell cycle, or intracellular signaling systems. Upregulated genes with apparent cell cycle function are listed in Table 4. The data discussed in this study have been deposited in NCBIs Gene Expression Omnibus (GEO, http://www.ncbi.nlm.nih.gov/geo/) and are accessible through GEO Series accession number GSE43066.

Real-time RT-PCR analysis

Expression levels of representative cell cycle-related genes selected from those listed in Table 4 were determined by real-time RT-PCR in the TAA and FB groups and compared with the untreated controls (Table 5). mRNA levels of all examined genes (*Cdkn2b, Cdkn1a, Ccnd1, Ccna2, Ccne2, Cdr2, Wee1, Tpx2, Gadd45a, Cdk1, Ccnb1, Aurkb,* and *Aurka*) were significantly increased in the TAA group as compared with the untreated controls. In addition, mRNA levels of *Cdkn2b, Cdkn1a, Ccnd1, Ccne2, Cdr2,* and *Cdk1* were also significantly increased in the FB group as compared with the untreated controls.

Cell proliferative activity and apoptosis

The nuclear antigen Ki-67 is a cell proliferation marker that is expressed in cells during the G_1 to M phase of the cell cycle (Scholzen and Gerdes 2000). The number of Ki-67$^+$ cells was significantly increased in the TAA, FB, and MEG groups as compared with the untreated controls, as previously reported (Taniai et al. 2012; Online Resource 2, Fig. s1A). A significant increase in Ki-67$^+$ cells was observed in the TAA and MEG groups as compared with the non-carcinogen groups (APAP and ANIT), while there was no difference in the number of Ki-67$^+$ cells in FB group compared with both non-carcinogen groups. PBO did not increase the number of Ki-67$^+$ proliferating cells.

TUNEL$^+$ cells were significantly increased in the TAA and MEG groups as compared with the untreated controls and non-carcinogen groups, as previously reported (Taniai et al. 2012; Online Resource 2, Fig. s1B). FB induced a significant increase in TUNEL$^+$ cells as compared with the APAP group. PBO did not increase the number of TUNEL$^+$ cells.

Immunoreactivity of G_1/S phase transition proteins

$p21^{Cip1}$ is a one of the Cyclin-dependent kinase (CDK) inhibitors that play a role in the G_1 checkpoint (Sherr and Roberts 1995). There was nuclear immunoreactivity for $p21^{Cip1}$ in the liver cells of untreated controls (Fig. 1a). The number of cells that was immunoreactive for $p21^{Cip1}$ was significantly increased in all carcinogen-treated groups as compared with the untreated controls and both non-carcinogen groups (Fig. 1a).

$p16^{Ink4a}$ and $p27^{Kip1}$, CDK inhibitors playing a role in the facilitation of the G_1 cell cycle arrest by binding to CDKs (Sherr and Roberts 1995), showed weak to moderate nuclear immunoreactivity in the liver cells of untreated controls. Strong nuclear and cytoplasmic immunoreactivity for $p16^{Ink4a}$ were found in the TAA group. Conversely, animals treated with other carcinogens or non-carcinogens only showed nuclear immunoreactivity. However, the number of immunoreactive cells was mostly unchanged by these treatments (Online Resource 2, Fig. s2A). The number of $p27^{Kip1+}$ cells did not statistically change in any of the carcinogen groups as compared with the untreated controls and non-carcinogen groups (Online Resource 2, Fig. s2B).

Immunoreactivity of G_2/M transition proteins

Cdc2, a molecule that drives the G_2/M transition in coordination with cyclin B1 (Chan et al. 1999), showed nuclear and/or cytoplasmic immunoreactivity in the liver cells of the untreated controls with the antibody recognizing both the phosphorylated and non-phosphorylated isoforms used here. Because Cdc2 is transported into the nucleus together with cyclin B1 upon activation (Chan et al. 1999), we counted cells showing nuclear immunoreactivity. Expression of nuclear Cdc2$^+$ cells significantly increased in the TAA, FB, and MEG groups as compared with the untreated controls and both non-carcinogen groups. However, PBO did not increase the number of nuclear Cdc2$^+$ cells (Fig. 1b).

Phospho-Wee1, acting at the G_2/M transition (Hashimoto et al. 2006), showed weak-to-moderate nuclear immunoreactivity in the liver cells of untreated controls. However, there were no specific expression changes in response to carcinogen treatment as compared with untreated controls or non-carcinogen groups (Online Resource 2, Fig. s2C).

Immunoreactivity of M phase proteins

Aurora B and Incenp, an interaction partner during mitosis (Ruchaud et al. 2007), were immunolocalized in the nuclei of the liver cells of untreated controls. Aurora B-immunoreactive cells were significantly increased in all carcinogen groups as compared with the untreated controls and the APAP group. In comparison with the ANIT group, Aurora B-immunoreactive cells significantly increased after treatment with FB, PBO, and MEG (Fig. 1c). Incenp-immunoreactive cells were significantly increased in all carcinogen groups as compared with the untreated controls and the ANIT group. However, APAP significantly increased Incenp$^+$ cells similar to the carcinogen groups (Fig. 1d). Phosphorylated-Histone H3 (p-Histone H3), the phosphorylated active isoform by Aurora B-kinase activity, causes heterochromatin protein 1α (HP1α) dissociation from heterochromatin, both acting at the early M phase (Hirota et al. 2005). Both p-Histone H3 and HP1α showed nuclear immunolocalization in the untreated controls. p-Histone H3$^+$ cells were significantly increased in the carcinogen groups as compared with the untreated controls and the APAP group. In comparison with the ANIT group, p-Histone H3 immunoreactive cells were significantly increased in the TAA, FB, and MEG groups (Fig. 1e). The number of HP1α^+ cells was significantly increased in the TAA, FB, and MEG groups as compared with the untreated controls. A significant increase in HP1α^+ cells was observed in the TAA and MEG groups as compared with the non-carcinogen groups, while the number of HP1α^+ cells in the FB group was statistically not different from those of the non-carcinogen groups. PBO did not increase HP1α^+ cells (Fig. 1f).

Expression of p53 and downstream Mdm2

Tp53 mRNA levels were significantly increased in the TAA group as compared with the untreated controls.

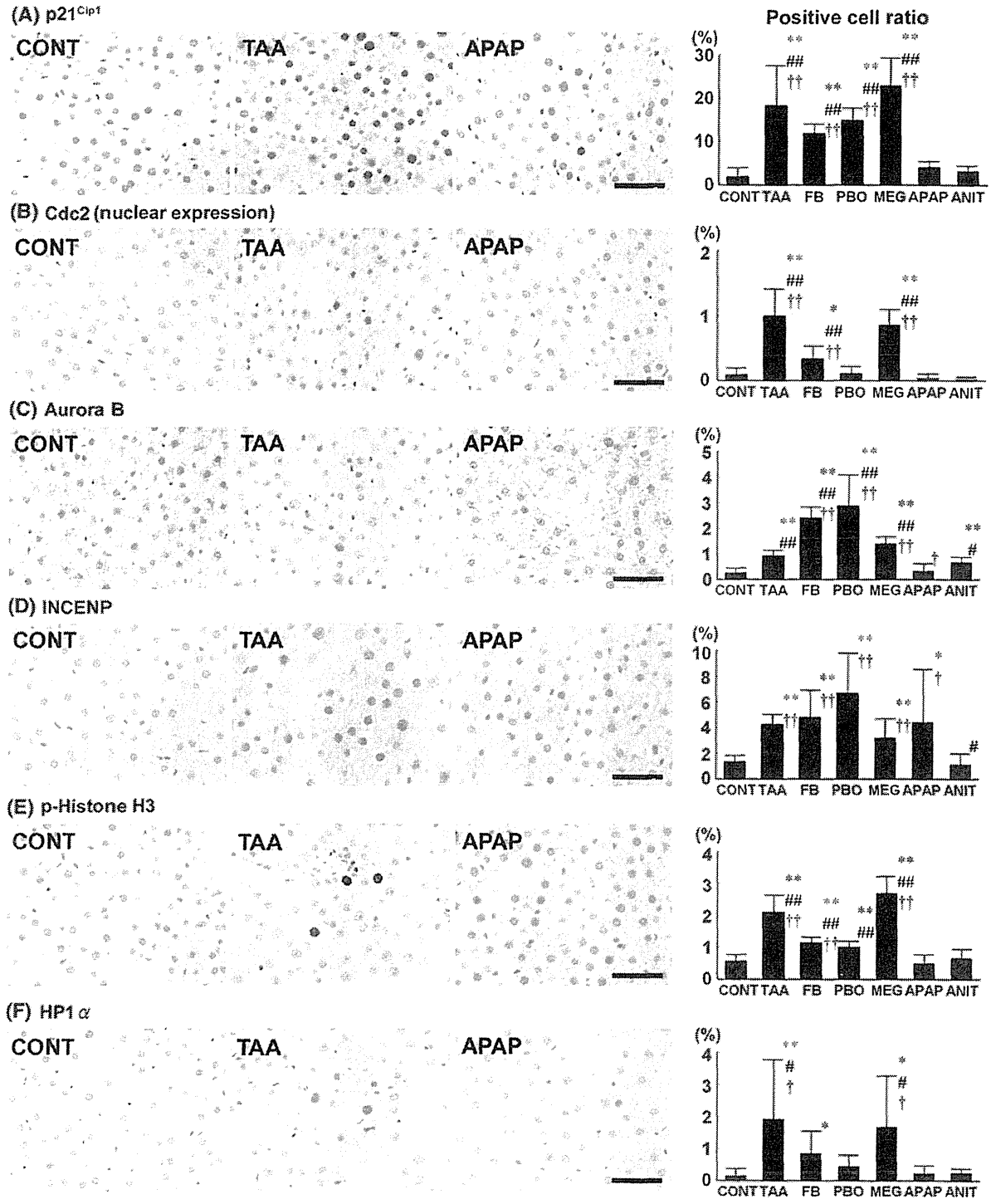

Fig. 1 Immunohistochemical cellular distribution of cell cycle proteins in liver cells after 28-day treatment with hepatocarcinogens or non-carcinogens in rats. Photomicrographs show distributions of $p21^{Cip1}$, nuclear Cdc2, Aurora B, Incenp, p-Histone H3, and HP1α immunoreactive cells in the livers of representative cases of an untreated control and animals treated with TAA or APAP. The graphs show positive cell ratios (%) of liver cells per total cells counted using 10 animals in each group. Values are presented as mean + SD (**a**) $p21^{Cip1}$, (**b**) Cdc2, (**c**) Aurora B, (**d**) Incenp, (**e**) p-Histone H3, and (**f**) HP1α. Magnification:×400 (*Bar* = 50 μm). *, ** $P < 0.05$, 0.01 versus untreated controls (Dunnett's or Steel's test). #, ## $P < 0.05$, 0.01 versus APAP (Dunnett's or Steel's test). †, †† $P < 0.05$, 0.01 versus ANIT (Dunnett's or Steel's test)

Table 4 Representative cell cycle-related genes with known functional annotations that were upregulated in the livers of rats treated with TAA (≥twofold)

Accession No.	Gene title	Symbol	TAA
XM_001054052	Anaphase promoting complex subunit 4	Anapc4	2.30
NM_153296	Aurora kinase A	Aurka	2.22
NM_053749	Aurora kinase B	Aurkb	4.03
XM_001080790	Cancer susceptibility candidate 5	Casc5	2.71
NM_053702	Cyclin A2	Ccna2	2.26
NM_171991	Cyclin B1	Ccnb1	4.16
NM_001009470	Cyclin B2	Ccnb2	2.45
NM_171992	Cyclin D1	Ccnd1	2.54
XM_001077331	Cyclin E1	Ccne1	3.80
XM_001064075	Cyclin E2	Ccne2	3.94
NM_012923	Cyclin G1	Ccng1	6.18
NM_019296	Cyclin-dependent kinase 1	Cdc2	2.52
XM_001068286	Cell division cycle associated 2	Cdca2	5.10
NM_001007648	Cell division cycle associated 3	Cdca3	2.93
NM_001025693	Cell division cycle associated 7	Cdca7	7.72
NM_001025050	Cell division cycle associated 8	Cdca8	2.92
NM_001012035	Cyclin-dependent kinase-like 2 (CDC2-related kinase)	Cdkl2	2.06
NM_080782	Cyclin-dependent kinase inhibitor 1A	Cdkn1a	5.96
NM_130812	Cyclin-dependent kinase inhibitor 2B (p15, inhibits CDK4)	Cdkn2b	2.52
NM_001025682	Cerebellar degeneration-related 2	Cdr2	5.90
XM_001069485	Centromere protein A	Cenpa	2.72
XM_001077739	Centromere protein E	Cenpe	2.78
NM_001008366	Centromere protein N	Cenpn	3.60
NM_001014215	Centromere protein Q	Cenpq	2.28
NM_001025646	Centrosomal protein 55	Cep55	2.20
NM_001017470	Centrosomal protein 70	Cep70	2.88
XM_001067027	Centrosomal protein 76	Cep76	3.34
XM_001076228	Centrosomal protein 135	Cep135	2.58
NM_080400	CHK1 checkpoint homolog (S. pombe)	Chek1	2.60
XM_001058264	Claspin homolog (Xenopus laevis)	Clspn	2.29
XM_001073486	Disks, large (Drosophila) homolog-associated protein 5	Dlgap5	2.68
XM_001070442	Excision repair cross-complementing rodent repair deficiency complementation group 6-like	Ercc6 l	2.11
XM_001067790	Extra spindle poles like 1 (S. cerevisiae)	Espl1	2.30
XM_001065873	F-box protein 5	Fbxo5	2.06
XM_001075601	Fizzy/cell division cycle 20 related 1 (Drosophila)	Fzr1	2.20
NM_024127	Growth arrest and DNA-damage-inducible, alpha	Gadd45a	2.54
NM_001008321	Growth arrest and DNA-damage-inducible, beta	Gadd45b	2.73
XM_001078275	G-2 and S-phase expressed 1	Gtse1	14.53
XM_001074188	Inner centromere protein	Incenp	3.37
XM_001065116	Kinesin family member 2A	Kif2a	4.79
NM_001085369	Kinesin family member 2C	Kif2c	2.10
XM_001061764	Kinesin family member 20A	Kif20a	2.43
XM_001070728	Minichromosome maintenance complex component 3	Mcm3	2.94
XM_001068436	Similar to mcdc21 protein; minichromosome maintenance complex component 4	Mcm4	2.50
NM_012603	Myelocytomatosis oncogene	Myc	3.30
XM_001055166	NIMA (never in mitosis gene a)-related expressed kinase 2	Nek2	2.07
NM_182953	NIMA (never in mitosis gene a)-related kinase 6	Nek6	2.34
NM_177931	Origin recognition complex, subunit 1-like (yeast)	Orc1 l	2.10

Table 4 continued

Accession No.	Gene title	Symbol	TAA
NM_199092	Origin recognition complex, subunit 4-like (yeast)	Orc4 l	2.53
NM_001033690	Origin recognition complex, subunit 6 like (yeast)	Orc6 l	2.19
NM 017198	p21 protein (Cdc42/Rac)-activated kinase 1	Pak1	2.90
NM_017100	Polo-like kinase 1 (Drosophila)	Plk1	3.24
NM_031821	Polo-like kinase 2 (Drosophila)	Plk2	3.41
NM_001007754	Ras association (RalGDS/AF-6) domain family member 1	Rassf1	2.43
XM_001055763	Retinoblastoma-like 1 (p107)	Rbl1	2.60
XM_001077474	SPC24, NDC80 kinetochore complex component, homolog (S. cerevisiae)	Spc24	4.70
NM_001009654	SPC25, NDC80 kinetochore complex component, homolog (S. cerevisiae)	Spc25	5.73
NM_022183	Topoisomerase (DNA) II alpha	Top2a	2.20
NM_001107790	TPX2, microtubule-associated, homolog (Xenopus laevis)	Tpx2	3.18
NM_001012742	Wee 1 homolog (S. pombe)	Wee1	6.38
NM_019376	Tyrosine 3-monooxygenase/tryptophan 5-monooxygenase activation protein, gamma polypeptide	Ywhag	2.30

Values are fold change with the expression level in the untreated control group set as 1

mRNA levels of *Mdm2*, a protein regulated by *Tp53*, were significantly increased in both TAA and FB groups as compared with the untreated controls (Fig. 2a).

Immunohistochemically, p53 showed nuclear immunolocalization in the untreated controls. Immunoreactive cells for p53 were significantly increased in the TAA, FB, and MEG groups as compared with the untreated controls and the non-carcinogen groups (Fig. 2b). However, PBO did not increase the number of $p53^{+}$ cells.

Real-time RT-PCR analysis of Ndrg1 and Klf6

Gene expression levels of N-myc downstream regulated gene 1 (*Ndrg1*) and Kruppel-like factor 6 (*Klf6*) were investigated in all hepatocarcinogen groups and compared with those of the untreated controls (Fig. 3). Transcript levels of *Ndrg1* significantly increased in the TAA group as compared with the untreated controls. Transcript levels of *Klf6* significantly increased in the TAA, PBO, and MEG groups as compared with the untreated controls. Transcript levels of *Klf6* were also non-significantly increased in the FB group (Fig. 3).

Discussion

We used microarrays to profile gene expression in the livers of rats treated with TAA for 28 days and found fluctuations in transcript levels of cell cycle-related genes. We then investigated the immunohistochemical cellular distribution of cell cycle proteins and reviewed the results along with the cell proliferation activity and apoptotic cell distribution that we previously studied in the livers of rats treated with hepatocarcinogens or non-hepatocarcinogenic hepatotoxicants (Taniai et al. 2012). We found that all hepatocarcinogens studied, irrespective of their cytomegaly inducing potential, increased cellular distribution of the G_1/S checkpoint protein $p21^{Cip1}$ and of the M phase proteins Aurora B and Incenp. We also found that hepatocarcinogens that induced high cell proliferation activity by increasing the number of $Ki\text{-}67^{+}$ cells induced increases in the cellular distribution of p53 and the M phase-related proteins nuclear Cdc2, p-Histone H3, and HP1α. These results suggest that hepatocarcinogens increased cell populations in the G_1/S checkpoint or M phase, and hepatocarcinogens that induced high cell proliferation activity also increased cell populations facilitating M phase arrest.

Repeated treatment of rats with chemical carcinogens often results in target cell proliferation (Tanaka et al. 2000; Lock and Hard 2004). We recently found that carcinogens that caused high cell proliferation activity, irrespective of the target organ, increased the population of cells co-expressing Topo IIα and ubiquitin D (Ubd) (Taniai et al. 2012). Topo IIα functions at the G_2/M transition (Wang et al. 2008), and overexpression of Ubd leads to chromosomal instability through reduction of kinetochore localization of the spindle assembly checkpoint protein Mad2 (Lim et al. 2006; Herrmann et al. 2007). In the present study, we found an increase in nuclear Cdc2-expressing liver cells similar to that of $Ki\text{-}67^{+}$ cells after treatment with three of the four hepatocarcinogens (TAA, FB and MEG). Cdc2 and cyclin B form the cyclin B-Cdc2 complex, which initiates the G_2/M transition, and nuclear localization of Cdc2 represents the active isoform entering at the M phase (Kawamoto et al. 1997; Chan et al. 1999). We previously found an increase in $Cdc2^{+}$ cells parallel to that of $Ki\text{-}67^{+}$ cells in the proliferative lesions in a

Table 5 Validations in transcript levels measured by real-time RT–PCR in the livers of rats treated with TAA or FB

Gene symbol	Real-time RT-PCR normalized by *Actb*	
	TAA[a]	FB[a]
Cdkn2b	4.32 ± 0.20[b]**	2.03 ± 0.57**
Cdkn1a	3.49 ± 1.02**	2.32 ± 0.69**
Ccnd1	2.73 ± 0.52**	1.79 ± 0.48*
Ccna2	3.06 ± 0.61**	1.56 ± 0.52
Ccne2	6.60 ± 2.11**	1.48 ± 0.33*
Cdr2	7.94 ± 2.01**	1.44 ± 0.25*
Wee1	4.99 ± 2.83*	1.18 ± 0.54
Tpx2	3.38 ± 0.28**	1.16 ± 0.28
Gadd45a	2.76 ± 0.80**	1.60 ± 0.62
Cdk1	2.69 ± 0.61**	1.64 ± 0.44*
Ccnb1	2.28 ± 0.59**	1.57 ± 0.50
Aurkb	2.75 ± 0.65**	1.34 ± 0.21
Aurka	2.85 ± 0.42**	1.27 ± 0.27

Aurk aurora kinase, *Ccn* cyclin, *Cdk* cyclin-dependent kinase, *Cdkn* cyclin-dependent kinase inhibitor, *Cdr2* cerebellar degeneration-related 2, *Gadd45a* growth arrest and DNA-damage-inducible, alpha, *Tpx2* microtubule-associated, homolog (*Xenopus laevis*), *Wee1* wee 1 homolog (*S. pombe*)

* $P < 0.05$ versus untreated controls

** $P < 0.01$ versus untreated controls

[a] Numbers of animals examined were 6 in each group

[b] Mean ± SD

two-stage thyroid carcinogenesis model, suggestive of cell proliferation activity (Ago et al. 2010). We also found an increased number of cells positive for p-Histone H3 and its interaction partner HP1α, acting at the early M phase (Hirota et al. 2005), after treatment with hepatocarcinogens that induce high cell proliferation activity. The only exception was an increase in p-Histone $H3^+$ cells after treatment with PBO without increased cell proliferation. It was previously reported that p-Histone H3 and HP1α reflect cell proliferation (De Koning et al. 2009; Aune et al. 2011). Together with our previous study results, these results suggest that carcinogens inducing high cell proliferation activity produce cell populations undergoing sustained activation of the G_2/M checkpoint, resulting in cells inappropriately exiting from the G_2/M checkpoint and undergoing M phase arrest.

Like nuclear Cdc2, p-Histone H3 and HP1α, Aurora B and its interaction partner Incenp are M phase proteins. The Aurora B-Incenp complex has a function in correcting chromosome attachments (Ruchaud et al. 2007). We found that all hepatocarcinogens studied increased the number of Aurora B^+ or $Incenp^+$ cells, irrespective of the potential for inducing cell proliferation, as compared with the untreated controls and non-carcinogenic APAP and ANIT. The exception was an increase in the $Incenp^+$ population caused by APAP. Overexpression of Aurora B causes chromosomal instability in various cancer cells (Qi et al. 2007). It was reported that aberrant expression of Incenp may cause chromosomal instability or its aberrant segregation in human breast cancer cells (Nguyen and Ravid 2006). Therefore, hepatocarcinogens may cause chromosomal instability at the early stages of hepatocarcinogenesis and hepatocarcinogens that induce cell proliferation further produce cells in M phase arrest.

In the present study, $p21^{Cip1+}$ cells specifically increased after treatment with hepatocarcinogens. We did not find fluctuations in immunoreactive cellular distribution of other CDK inhibitors such as $p16^{Ink4a}$ and $p27^{Kip1}$ specific to hepatocarcinogens. Expression of $p21^{Cip1}$ is usually regulated by p53 to mediate G_1 arrest (Sherr and Roberts 1995). While the cellular distribution pattern of $p21^{Cip1}$ was similar to that of p53 after treatment with TAA, FB, and MEG, p53 did not respond to PBO in the present study. It is reported that there are a number of p53-independent mechanisms for $p21^{Cip1}$ induction (Abbas and Dutta 2009). There are a number of p53-independent $p21^{Cip1}$ inducers, such as Ndrg1 and Klf6 (Abbas and Dutta 2009; Kovacevic et al. 2011). In the present study, expression of both *Ndrg1* and *Klf6* was found to be upregulated by TAA-treatment, as shown by microarray analysis. We further found upregulation of *Klf6* by three of the four hepatocarcinogens (TAA, PBO and MEG) by real-time RT-PCR analysis as compared with untreated control animals. Therefore, it is possible that 28-day treatment with hepatocarcinogens produces cell populations arrested at the G_1 phase by $p21^{Cip1}$ via a mechanism independent of p53.

In the present study, transcript levels of *p53* and *Mdm2* significantly increased in the TAA group. $p53^+$ cells were increased after treatment with hepatocarcinogens that induced cell proliferation. It is well known that p53 induces apoptosis in response to DNA damage (Gotz and Montenarh 1995). We previously demonstrated that hepatocarcinogens that induced cell proliferation also induce apoptosis of liver cells (Taniai et al. 2012). These results suggest that hepatocarcinogens that induce cell proliferation also activate the p53 signaling cascade in response to G_1 or M phase arrest to undergo apoptosis. An increase in Mdm2 transcripts may represent facilitation of metabolic turnover of p53 (Fuchs et al. 1998).

With regard to the difference in the cellular responses on M phase proteins between PBO and other hepatocarcinogens, we think cellular responses may be parallel to the cell proliferation potential of carcinogens. It has been proposed that a non-genotoxic mode of action to induce hepatocellular apoptosis with subsequent regeneration (proliferation) is responsible for the hepatocarcinogenicity of fumonisin B_1 mycotoxin (Dragan et al. 2001). We recently found increased proliferation and apoptosis of liver cells

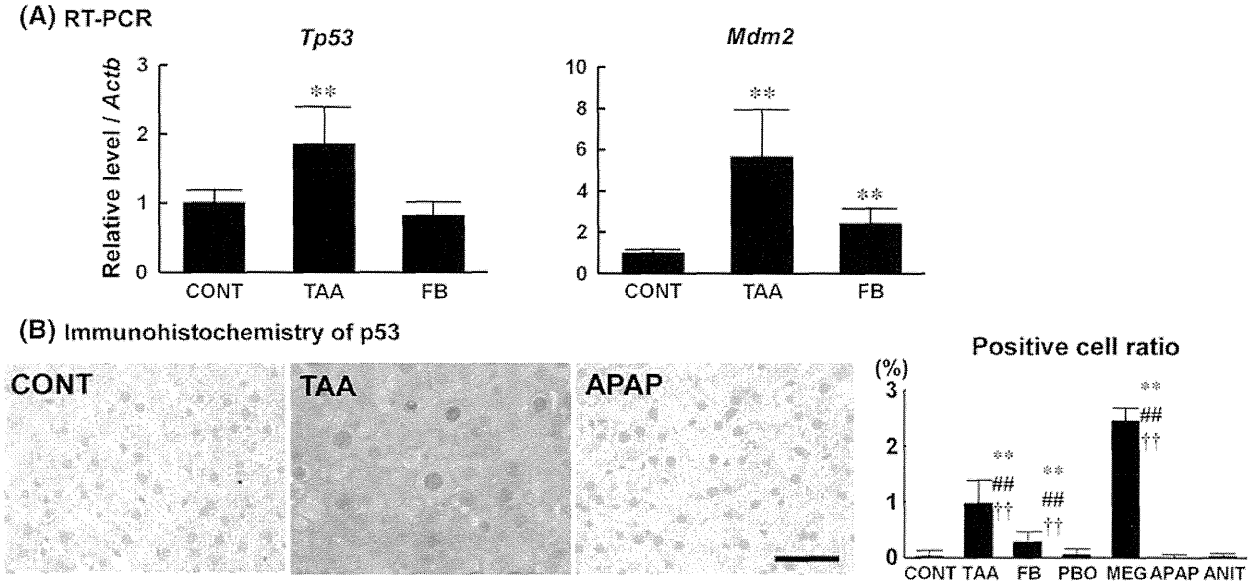

Fig. 2 Expression of p53 and downstream Mdm2 in the liver after 28-day treatment with hepatocarcinogens in rats. **a** Real-time RT-PCR analysis of p53 and Mdm2. Values are expressed as group mean fold changes over untreated controls. Values represent mean + SD *, ** $P < 0.05$, 0.01 versus untreated controls (Dunnett's or Steel's test). **b** Immunohistochemical cellular distribution of p53 in liver cells. Photomicrographs show immunoreactive cell distributions of p53 in the liver cells in representative cases of an untreated control and animals treated with TAA or APAP. The graphs show positive cell ratios (%) of liver cells per total cells counted using 10 animals in each group. Magnification: ×400 (*Bar* = 50 μm). ** $P < 0.01$ versus untreated controls (Dunnett's or Steel's test). ## $P < 0.01$ versus APAP (Dunnett's or Steel's test). †† $P < 0.01$ versus ANIT (Dunnett's or Steel's test)

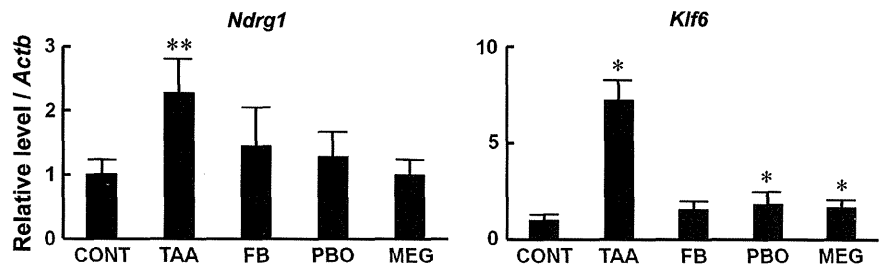

Fig. 3 Real-time RT-PCR analysis of *Ndrg1* and *Klf6*. Values are expressed as group mean fold changes over untreated controls. Numbers of animals examined were 6 in each group. Values represent mean + SD *, ** $P < 0.05$, 0.01 versus untreated controls (Dunnett's or Steel's test)

following treatment with either TAA, FB, or MEG; however, we did not find increased proliferation or apoptosis after PBO treatment (Taniai et al. 2012). It may be reasonable to hypothesize that induction of proliferation and apoptosis in carcinogenic target cells is dependent on carcinogenic potential of chemicals administered. It is well known that tumor-promoting potential of hepatocarcinogens in a rat two-stage hepatocarcinogenesis model correlates well with their hepatocarcinogenic potential (Shirai 1997). We previously reported that TAA and FB had higher tumor promoting activity than PBO (Ichimura et al. 2010), with the dose level used in the present study. MEG induces hepatocellular adenomas and carcinomas in rats after repeated oral administration at 300 mg/kg/day even at the one-year interim killing in two-year carcinogenesis test (NTP 2000). This dose is less than one-third of the dose level in the present study. Therefore, the lack of cellular responses to some M phase proteins with PBO may be a reflection of its weaker carcinogenic potential as compared with TAA, FB, and MEG.

In conclusion, hepatocarcinogens, irrespective of their cytomegaly inducing potential, increased the population of $p21^{Cip1+}$ cells, suggesting production of a cell population arrested at the G_1 phase by $p21^{Cip1}$. All hepatocarcinogens studied also increased Aurora B^+ and $Incenp^+$ cells, suggesting an increased cell population with chromosomal instability. Hepatocarcinogens that induced cell proliferation further increased the number of immunoreactive cells for p53, nuclear Cdc2, p-Histone H3, and HP1α, suggesting that cell cycle facilitation may cause M phase arrest accompanied by apoptosis. Therefore, the present study indicates that a combination of these proteins may be an early prediction marker of hepatocarcinogens in a 28-day treatment scheme in rats.

Acknowledgments The authors thank Mrs. Shigeko Suzuki for her technical assistance in preparing the histological specimens. This work was supported by Health and Labour Sciences Research Grants (Research on Food Safety) from the Ministry of Health, Labour and Welfare of Japan.

Conflict of interest The authors disclose that there are no competing financial interests that could inappropriately influence the outcome of this study.

References

Abbas T, Dutta A (2009) p21 in cancer: intricate networks and multiple activities. Nat Rev Cancer 9:400–414

Adler M, Müller K, Rached E, Dekant W, Mally A (2009) Modulation of key regulators of mitosis linked to chromosomal instability is an early event in ochratoxin A carcinogenicity. Carcinogenesis 30:711–719

Ago K, Saegusa Y, Nishimura J, Dewa Y, Kemmochi S, Kawai M, Harada T, Mitsumori K, Shibutani M (2010) Involvement of glycogen synthase kinase-3beta signaling and aberrant nucleocytoplasmic localization of retinoblastoma protein in tumor promotion in a rat two-stage thyroid carcinogenesis model. Exp Toxicol Pathol 62:269–280

Allen DG, Pearse G, Haseman JK, Maronpot RR (2004) Prediction of rodent carcinogenesis: an evaluation of prechronic liver lesions as forecasters of liver tumors in NTP carcinogenicity studies. Toxicol Pathol 32:393–401

Aune G, Stunes AK, Tingulstad S, Salvesen O, Syversen U, Torp SH (2011) The proliferation markers Ki-67/MIB-1, phosphohistone H3, and survivin may contribute in the identification of aggressive ovarian carcinomas. Int J Clin Exp Pathol 4:444–453

Becker FF (1983) Thioacetamide hepatocarcinogenesis. J Natl Cancer Inst 71:553–558

Chan TA, Hermeking H, Lengauer C, Kinzler KW, Vogelstein B (1999) 14-3-3σ is required to prevent mitotic catastrophe after DNA damage. Nature 401:616–620

Clawson GA, Blankenship LJ, Rhame JG, Wilkinson DS (1992) Nuclear enlargement induced by hepatocarcinogens alters ploidy. Cancer Res 52:1304–1308

De Koning L, Savignoni A, Boumendil C, Rehman H, Asselain B, Sastre-Garau X, Almouzni G (2009) Heterochromatin protein 1alpha: a hallmark of cell proliferation relevant to clinical oncology. EMBO Mol Med 1:178–191

Dragan YP, Bidlack WR, Cohen SM, Goldsworthy TL, Hard GC, Howard PC, Riley RT, Voss KA (2001) Implications of apoptosis for toxicity, carcinogenicity, and risk assessment: fumonisin B1 as an example. Toxicol Sci 61:6–17

Eastin WC (1998) The U.S. National toxicology program evaluation of transgenic mice as predictive models for identifying carcinogens. Environ Health Perspect 106:81–84

Fuchs SY, Adler V, Buschmann T, Wu X, Ronai Z (1998) Mdm2 association with p53 targets its ubiquitination. Oncogene 17:2543–2547

Gotz C, Montenarh M (1995) P53 and its implication in apoptosis (review). Int J Oncol 6:1129–1135

Hamadeh HK, Jayadev S, Gaillard ET, Huang Q, Stoll R, Blanchard K, Chou J, Tucker CJ, Collins J, Maronpot R, Bushel P, Afshari CA (2004) Integration of clinical and gene expression endpoints to explore furan-mediated hepatotoxicity. Mutat Res 18:169–183

Hashimoto O, Shinkawa M, Torimura T, Nakamura T, Selvendiran K, Sakamoto M, Koga H, Ueno T, Sata M (2006) Cell cycle regulation by the Wee1 inhibitor PD0166285, pyrido [2,3-d] pyrimidine, in the B16 mouse melanoma cell line. BMC Cancer 6:292

Herrmann J, Lerman LO, Lerman A (2007) Ubiquitin and ubiquitin-like proteins in protein regulation. Circ Res 100:1276–1291

Hirota T, Lipp JL, Tof BH, Peters JM (2005) Histone H3 serine 10 phosphorylation by Aurora B causes HP1 dissociation from heterochromatin. Nature 438:1176–1180

Ichijima Y, Yoshioka K, Yoshioka Y, Shinohe K, Fujimori H, Unno J, Takagi M, Goto H, Inagaki M, Mizutani S, Teraoka H (2010) DNA lesions induced by replication stress trigger mitotic aberration and tetraploidy development. PLoS ONE 5:e8821

Ichimura R, Mizukami S, Takahashi M, Taniai E, Kemmochi S, Mitsumori K, Shibutani M (2010) Disruption of Smad-dependent signaling for growth of GST-P-positive lesions from the early stage in a rat two-stage hepatocarcinogenesis model. Toxicol Appl Pharmacol 246:128–140

Irizarry RA, Hobbs B, Collin F, Beazer-Barclay YD, Antonellis KJ, Scherf U, Speed TP (2003) Exploration, normalization, and summaries of high density oligonucleotide array probe level data. Biostatistics 4:249–264

Kawamoto H, Koizumi H, Uchikoshi T (1997) Expression of the G_2-M checkpoint regulators cyclin B1 and cdc2 in nonmalignant and malignant human breast lesions: immunocytochemical and quantitative image analyses. Am J Pathol 150:15–23

Kovacevic Z, Sivagurunathan S, Mangs H, Chikhani S, Zhang D, Richardson DR (2011) The metastasis suppressor, *N*-myc downstream regulated gene 1 (NDRG1), upregulates p21 via p53-independent mechanisms. Carcinogenesis 32:732–740

Lim CB, Zhang D, Lee CG (2006) FAT10, a gene up-regulated in various cancers, is cell-cycle regulated. Cell Div 1:20

Livak KJ, Schmittgen TD (2001) Analysis of relative gene expression data using real-time quantitative PCR and the $2^{-\Delta\Delta C_T}$ method. Methods 25:402–408

Lock EA, Hard GC (2004) Chemically induced renal tubule tumors in the laboratory rat and mouse: review of the NCI/NTP database and categorization of renal carcinogens based on mechanistic information. Crit Rev Toxicol 34:211–299

Muguruma M, Unami A, Kanki M, Kuroiwa Y, Nishimura J, Dewa Y, Umemura T, Oishi Y, Mitsumori K (2007) Possible involvement of oxidative stress in piperonyl butoxide induced hepatocarcinogenesis in rats. Toxicology 236:61–75

Nguyen HG, Ravid K (2006) Tetraploidy/aneuploidy and stem cells in cancer promotion: the role of chromosome passenger proteins. J Cell Physiol 208:12–22

NTP (1993) NTP Toxicology and Carcinogenesis Studies of Acetaminophen (CAS No. 103–90-2) in F344 Rats and B6C3F1 Mice (Feed Studies). Natl Toxicol Program Tech Rep Ser 394:1–274

NTP (2000) Toxicology and carcinogenesis studies of methyleugenol (CAS NO. 93–15-2) in F344/N rats and B6C3F1 mice (gavage studies). Natl Toxicol Program Tech Rep Ser 491:1–412

Qi G, Ogawa I, Kudo Y, Miyauchi M, Siriwardena BS, Shimamoto F, Tatsuka M, Takata T (2007) Aurora-B expression and its correlation with cell proliferation and metastasis in oral cancer. Virchows Arch 450:297–302

Rees KR, Rowland GF, Ross HF (1962) The metabolism of isolated rat-liver nuclei during chemical carcinogenesis. 2. 2-Acetylamidofluorene, a-naphthyl isothiocyanate and 2′, 4′-dimethyl-4-dimethylaminoazobenzene. Biochem J 82:347–352

Ruchaud S, Carmena M, Earnshaw WC (2007) Chromosomal passengers: conducting cell division. Nat Rev Mol Cell Biol 8:798–812

Scholzen T, Gerdes J (2000) The Ki-67 protein: from the known and the unknown. J Cell Physiol 182:311–322

Sherr CJ, Roberts JM (1995) Inhibitors of mammalian G_1 cyclin-dependent kinases. Genes Dev 9:1149–1163

Shirai T (1997) A medium-term rat liver bioassay as a rapid in vivo test for carcinogenic potential, a historical review of model development and summary of results from 291 tests. Toxicol Pathol 25:453–460

Shoda T, Onodera H, Takeda M, Uneyama C, Imazawa T, Takegawa K, Yasuhara K, Watanabe T, Hirose M, Mitsumori K (1999) Liver tumor promoting effects of Fenbendazole in rats. Toxicol Pathol 27:553–562

Takahashi O, Oishi S, Fujitani T, Tanaka T, Yoneyama M (1994) Chronic toxicity studies of piperonyl butoxide in F344 rats: induction of hepatocellular carcinoma. Fundam Appl Toxicol 22:293–303

Tamano S (2010) Carcinogenesis risk assessment of chemicals using medium-term carcinogenesis bioassays. Asian Pacific J Cancer Prev 11:4–5

Tanaka T, Kohno H, Murakami M, Shimada R, Kagami S (2000) Colitis-related rat colon carcinogenesis induced by 1-hydroxyanthraquinone and methylazoxymethanol acetate. Oncol Rep 7:501–508

Taniai E, Yafune A, Hayashi H, Itahashi M, Hara-Kudo Y, Suzuki K, Mitsumori K, Shibutani M (2012) Aberrant activation of ubiquitin D at G_2 phase and apoptosis by carcinogens that evoke cell proliferation after 28-day administration in rats. J Toxicol Sci 37:1093–1111

Uehara T, Minowa Y, Morikawa Y, Kondo C, Maruyama T, Kato I, Nakatsu N, Igarashi Y, Ono A, Hayashi H, Mitsumori K, Yamada H, Ohno Y, Urushidani T (2011) Prediction model of potential hepatocarcinogenicity of rat hepatocarcinogens using a large-scale toxicogenomics database. Toxicol Appl Pharmacol 255:297–306

Wang Y, Azuma Y, Moore D, Osheroff N, Neufeld KL (2008) Interaction between tumor suppressor adenomatous polyposis coli and topoisomerase IIα: implication for the G_2/M transition. Mol Biol Cell 19:4076–4085

Williams GM, Iatropoulos MJ, Jeffrey AM, Shirai T (2002) Protective effect of acetaminophen against colon cancer initiation effects of 3,2′-dimethyl-4-aminobiphenyl in rats. Eur J Cancer Prev 11:39–48

Toxicology Letters 219 (2013) 203–210

Contents lists available at SciVerse ScienceDirect

Toxicology Letters

journal homepage: www.elsevier.com/locate/toxlet

Aberrant activation of M phase proteins by cell proliferation-evoking carcinogens after 28-day administration in rats

Atsunori Yafune[a,b], Eriko Taniai[a,b], Reiko Morita[a,b], Hitomi Hayashi[a,b], Kazuhiko Suzuki[a], Kunitoshi Mitsumori[a], Makoto Shibutani[a,*]

[a] Laboratory of Veterinary Pathology, Tokyo University of Agriculture and Technology, 3-5-8 Saiwai-cho, Fuchu-shi, Tokyo 183-8509, Japan
[b] Pathogenetic Veterinary Science, United Graduate School of Veterinary Sciences, Gifu University, 1-1 Yanagido, Gifu-shi, Gifu 501-1193, Japan

HIGHLIGHTS

- This study aimed to identify early prediction markers of carcinogens in rats.
- Cellular distribution of cell cycle proteins was analyzed after 28-day treatment.
- Cell proliferation-evoking carcinogens induced activation of M phase proteins.
- Carcinogens lacking proliferative activity did not have these effects.
- Cell proliferation and M phase proteins might functions as an early prediction unit.

ARTICLE INFO

Article history:
Received 19 January 2013
Received in revised form 12 March 2013
Accepted 15 March 2013
Available online 25 March 2013

Keywords:
Carcinogen
M phase
Cell proliferation
Immunohistochemical analysis

ABSTRACT

We have previously reported that hepatocarcinogens increase liver cells expressing $p21^{Cip1}$, a G_1 checkpoint protein and M phase proteins after 28-day treatment in rats. This study aimed to identify early prediction markers of carcinogens available in many target organs after 28-day treatment in rats. Immunohistochemical analysis was performed on Ki-67, $p21^{Cip1}$ and M phase proteins [nuclear Cdc2, phospho-Histone H3 (p-Histone H3), Aurora B and heterochromatin protein 1α (HP1α)] with carcinogens targeting different organs. Carcinogens targeting thyroid (sulfadimethoxine; SDM), urinary bladder (phenylethyl isothiocyanate), forestomach (butylated hydroxyanisole; BHA), glandular stomach (catechol; CC), and colon (2-amino-1-methyl-6-phenylimidazo[4,5-*b*]pyridine and chenodeoxycholic acid) were examined using a non-carcinogenic toxicant (caprolactam) and carcinogens targeting other organs as negative controls. All carcinogens increased $Ki\text{-}67^+$, nuclear $Cdc2^+$, p-Histone $H3^+$ or Aurora B^+ carcinogenic target cells, except for both colon carcinogens, which did not increase cell proliferation. On the other hand, $p21^{Cip1+}$ cells increased with SDM and CC. HP1α responded only to BHA. Results revealed carcinogens evoking cell proliferation concurrently induced cell cycle arrest at M phase or showing chromosomal instability reflecting aberration in cell cycle regulation, irrespective of target organs, after 28-day treatment. Therefore, M phase proteins may be early prediction markers of carcinogens evoking cell proliferation in many target organs.

1. Introduction

In general, the method for evaluating carcinogenicity is a bioassay in which rodents are treated with a chemical for their entire 1.5- or 2-year lifespan. Carcinogenicity studies using experimental animals are time-consuming, expensive, and use many animals. However, there is no commonly rapid means for evaluating the carcinogenic potential of chemicals. Alternative animal models using medium-term carcinogenesis models (Tamano, 2010) or genetically modified animals using transgenic or gene-targeting technologies (Eastin, 1998) are also expensive and time-consuming or have limited target organs. Toxicogenomic approaches for the prediction of carcinogenic potential in each target organ appear promising. However, they are also expensive and require some integrative methodologies between different laboratories sharing an expression database (Uehara et al., 2011).

Development of nuclear enlargement is sometimes observed in carcinogenic target cells after repeated administration of

Abbreviations: SDM, sulfadimethoxine; PEITC, phenylethyl isothiocyanate; BHA, butylated hydroxyanisole; CC, catechol; PhIP, 2-amino-1-methyl-6-phenylimidazo[4,5-*b*]pyridine; CDCA, chenodeoxycholic acid; p-Histone H3, phospho-Histone H3; HP1α, heterochromatin protein 1α; CL, caprolactam.

* Corresponding author. Tel.: +81 42 367 5771; fax: +81 42 367 5771.
E-mail address: mshibuta@cc.tuat.ac.jp (M. Shibutani).

0378-4274/$ – see front matter © 2013 Elsevier Ireland Ltd. All rights reserved.
http://dx.doi.org/10.1016/j.toxlet.2013.03.012

carcinogens, irrespective of genotoxic potential, from the early stages of exposure in experimental animals (Adler et al., 2009; Allen et al., 2004). This nuclear enlargement is typically observed in the liver and kidney. It is often termed cytomegaly in cases of liver cells characterized by the presence of hepatocytes that are enlarged because of increased cytoplasmic volume, and karyomegaly when it occurs in renal tubular cells. Recent studies have shown that ochratoxin A, a representative renal carcinogen that can typically induce karyomegaly, induces aberrant expression of cell cycle-related proteins in the proximal tubular areas of the outer stripe of the outer medulla with karyomegaly (Adler et al., 2009). Generation of karyomegaly/cytomegaly suggests cell cycle aberration causing chromosomal instability through nuclear division during mitosis. Aberrant mitosis, such as chromosomal missegregation and cytokinesis failure occurring as a result of checkpoint dysfunction of the cell cycle, can induce tetraploidy/aneuploidy (Ichijima et al., 2010). This suggests that this aberrant expression of cell cycle-related proteins may eventually cause carcinogenicity in association with the development of chromosomal instability. Therefore, we hypothesize that an early event, which disrupts cell cycle regulation, triggers the carcinogenic response in the molecular mechanism responsible for the development of cytomegaly/karyomegaly.

We have previously analyzed cell cycle-related proteins in a 28-day study of repeated hepatocarcinogen administration to induce cytomegaly in rats (Yafune et al., 2013). These responses suggested hepatocarcinogens, irrespective of cytomegaly-inducing potential, induced an increase in the liver cell population immunoreactive for $p21^{Cip1}$ and Aurora B, suggestive of those undergoing G_1 arrest and chromosomal instability, respectively. We also found that hepatocarcinogens that evoke cell proliferation might cause M phase arrest of liver cells, judging from increased cell population expressing nuclear Cdc2, phospho-Histone H3 (p-Histone H3), and heterochromatin protein 1α (HP1α), accompanied with apoptosis. The obtained results suggested that a combination of these cell cycle proteins might be an early prediction battery of markers of hepatocarcinogens in a 28-day treatment scheme in rats.

There is a need for an available prediction tool to assess the carcinogenic potential of chemicals. To establish a short-term carcinogenicity screening system, it is reasonable to focus on common cellular responses in specific target organs. In the present study, based on our previous results on hepatocarcinogens, expression of these candidate proteins was explored in other target organs, including the thyroid, urinary bladder, forestomach, glandular stomach and colon, after 28-day treatment with organ-specific carcinogens in rats.

2. Materials and methods

2.1. Chemicals

Butylated hydroxyanisole (BHA; CAS No. 25013-16-5, ≥98.0%), caprolactam (CL; CAS No. 105-60-2, 98%), and catechol (CC; CAS No. 120-80-9, >99.0%) were purchased from Wako Pure Chemicals Industries, Ltd. (Osaka, Japan). Chenodeoxycholic acid (CDCA; CAS No. 474-25-9, ≥98.0%) and phenylethyl isothiocyanate (PEITC; CAS No. 2257-09-2, ≥97.0%) were obtained from Tokyo Chemical Industry Corporation (Tokyo, Japan). Sulfadimethoxine sodium salt (SDM; CAS No. 122-11-2) was obtained from Sigma–Aldrich Corporation (St. Louis, MO, USA). 2-Amino-1-methyl-6-phenylimidazo[4,5-*b*]pyridine (PhIP; CAS No. 105650-23-5, ≥98.0%) was obtained from Nard Institute (Hyogo, Japan).

2.2. Animal experiments

Five-week-old male F344/NSlc rats were purchased from Japan SLC, Inc. (Shizuoka, Japan) and acclimatized to a powdered basal diet (CRF-1 diet; Oriental Yeast Co., Tokyo, Japan) and tap water *ad libitum*. They were housed in stainless steel cages in a barrier-maintained animal room on a 12 h light–dark cycle and conditioned at 23 ± 3 °C with relative humidity of 50 ± 20%. After a 1-week acclimatization period, animals were randomized into groups of 10 each and treated with carcinogens or non-carcinogens for 28 days.

Animals were treated with carcinogenic doses of carcinogens targeting either the thyroid, urinary bladder, forestomach, glandular stomach or colon for 28 days. Groups received either SDM (1000 ppm in drinking water) targeting the thyroid, PEITC (1000 ppm in diet) targeting the urinary bladder, BHA (20,000 ppm in diet) targeting the forestomach, CC (8000 ppm in diet) targeting the glandular stomach, or CDCA (1000 ppm in diet) or PhIP (400 ppm in diet) targeting the colon. The dose of SDM and CDCA has been shown to promote carcinogenesis in the thyroid and colon, respectively, in rats (Ghia et al., 1996; Imai et al., 2004). With regard to PEITC, BHA, CC and PhIP, the dose has been shown to induce tumors in each target organ (Hagiwara et al., 2001; Ito et al., 1991; Kaneko et al., 2002; Sugiura et al., 2003). CL (10,000 ppm in diet) was selected as a non-carcinogenic control compound, exhibiting positivity in some genotoxicity studies (IARC, 1999). This compound has shown no carcinogenic effect in any organs with ≥7500 ppm in diet (Fukushima et al., 1991; NTP, 1982). Untreated control animals were given basal diet and tap water *ad libitum* for 28 days.

One day after the 28-day treatment, all animals were sacrificed by exsanguination from the abdominal aorta under deep anesthesia using CO_2/O_2, and target organs were removed. Target organs were fixed with 4% paraformaldehyde in 0.1 M sodium phosphate buffer solution (pH 7.4; Wako Pure Chemicals Industries, Ltd.). At necropsy, the urinary bladder was inflated by transurethral instillation of a paraformaldehyde solution, and the stomach and colon were instilled with a paraformaldehyde solution to facilitate mucosal fixation. The following samples were taken from fixed tissues and prepared for paraffin embedding: bilateral lobes of the thyroid; two longitudinal slices of the urinary bladder; three longitudinal slices of the stomach including forestomach and glandular stomach; and three cross cut pieces each from proximal, medial, and distal portions of the colon.

All procedures in this study were conducted in compliance with the Guidelines for Proper Conduct of Animal Experiments (Science Council of Japan, June 1, 2006) and according to the protocol approved by the Animal Care and Use Committee of the Tokyo University of Agriculture and Technology.

2.3. Histopathology and immunohistochemistry

Three micrometer sections of paraffin-embedded tissues from the thyroid, urinary bladder, stomach, and colon were stained with hematoxylin and eosin for histopathological examination and subjected to immunohistochemistry.

Immunohistochemistry was performed using the Vectastain® Elite ABC Kit (Vector Laboratories Inc., Burlingame, CA, USA) with 3,3′-diaminobenzidine/H_2O_2 as the chromogen. The following primary antibodies were used: Ki-67 (mouse monoclonal antibody, 1:50; Dako, Glostrup, Denmark), $p21^{Cip1}$ (mouse monoclonal antibody, 1:100; Abcam, Cambridge, UK), Cdc2 (mouse monoclonal antibody, 1:100; Santa Cruz Biotechnology, Inc., Santa Cruz, CA, USA), Aurora B (rabbit polyclonal antibody, 1:200; Abcam), p-Histone H3 (Ser 10 phosphorylated; rabbit polyclonal antibody, 1:50; Santa Cruz Biotechnology, Inc.), and HP1α (rabbit polyclonal antibody, 1:200; Cell Signaling Technology, Inc., Danvers, MA, USA). These antigens were selected based on our previous results (Yafune et al., 2013). Antigen retrieval was performed in an autoclave for 10 min at 121 °C in 10 mM citrate buffer (pH 6.0) for Ki-67 and p-Histone H3 and in a microwave for 10 min at 90 °C in 10 mM citrate buffer (pH 6.0) for $p21^{Cip1}$ and HP1α. Sections were counterstained with hematoxylin for microscopic examination.

2.4. Analysis of immunoreactivity

In the thyroid and urinary bladder, immunostained cells in the follicular area (thyroid) and mucosal area (urinary bladder) were counted in eight randomly selected areas per animal (four areas per tissue section) at magnifications of 400× in the former and 200× in the latter. In the forestomach, because cells immunoreactive for Ki-67, Aurora B, or HP1α were diffusely distributed in the basal cell layer, vertical length of positive cell distribution from the basement membrane was measured in 10 randomly selected areas per animal at 200× magnification. $p21^{Cip1+}$, nuclear $Cdc2^+$ or p-Histone $H3^+$ cells in the forestomach were counted in 10 randomly selected areas in the mucosa per animal at 200× magnification. In the glandular stomach, immunoreactive cells were counted in 10 randomly selected glands per animal at 200× magnification. In the colon, immunoreactive cells were counted in 10 randomly selected crypts per animal that were located close to the lamina muscularis mucosa and demonstrated a cross sectional view at 200× magnification.

Total cells were measured by counting all nuclei in each selected field in the thyroid and urinary bladder mucosa using WinROOF image analysis and measurement software (version 6.4.2., Mitani Corporation, Fukui, Japan). The percentage of immunoreactive cells was determined in each field. In the forestomach, mean vertical length of the distribution of Ki-67^+, Aurora B^+ or HP1α$^+$ cells within the mucosa was estimated from 10 fields and expressed as vertical length (μm). $p21^{Cip1+}$, nuclear $Cdc2^+$ or p-Histone $H3^+$ cell counts were expressed as numbers per 1000 μm of epithelial layer length in each field. In the glandular stomach, mean number of immunoreactive cells of 10 glands/animal was estimated and expressed as cells per gland. In the colon, percentage of immunoreactive cells was determined in each crypt by selecting 10 glands using WinROOF image analysis and measurement software.

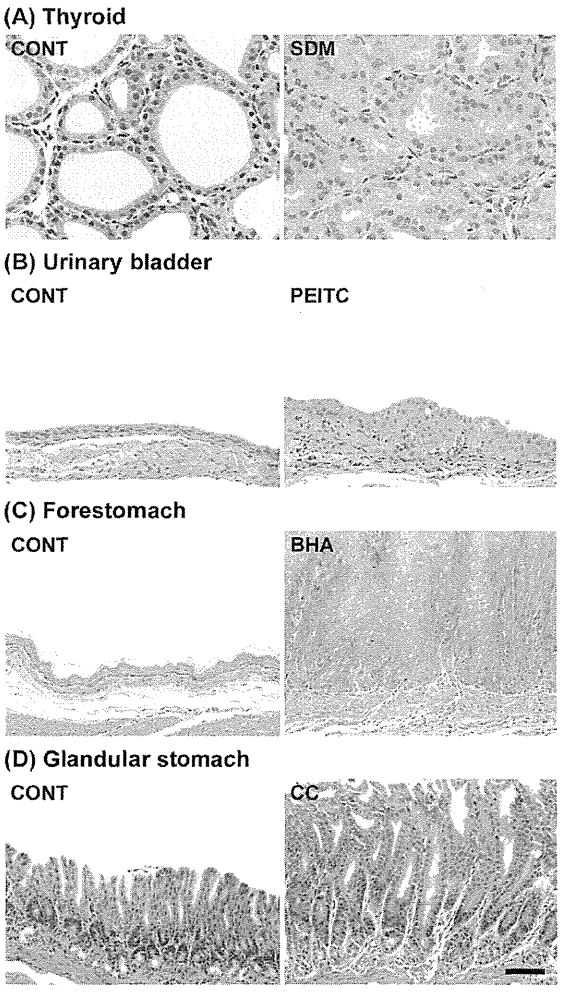

Fig. 1. Histopathological changes of the thyroid, urinary bladder, forestomach and glandular stomach in animals treated with SDM, PEITC, BHA and CC, respectively. (A) Thyroid, (B) urinary bladder, (C) forestomach and (D) glandular stomach. Bar = 50 μm (A). Bar = 100 μm (B–D).

2.5. Statistical analysis

Values for immunohistochemical cellular distribution in the thyroid, urinary bladder, forestomach, glandular stomach and colon were analyzed by Student's *t*-test with Bonferroni correction. A p values of less than 0.0056 (thyroid and urinary bladder), 0.0071 (forestomach and glandular stomach) and 0.0045 (colon) were regarded as statistically significant. Results were compared among all treatment groups and the untreated controls. Comparison between each carcinogen group in specific target organ and non-carcinogenic CL or other carcinogen groups targeting other organs was similarly performed, excluding the untreated control group from comparison. In the colon, comparison between carcinogen group targeting organ (PhIP or CDCA) and other treatment groups was similarly performed, excluding the untreated control group and PhIP or CDCA from comparison.

3. Results

3.1. Histopathological changes

Treatment with SDM resulted in scant colloidal fluid and follicular epithelial cell proliferation in the thyroid (Fig. 1A), leading to the formation of small follicles consisting of large cuboidal cells, similar to previous findings (Imai et al., 2004). Treatment with PEITC resulted in scattered foci of simple hyperplasia or papillary and nodular hyperplasia of the epithelia in the urinary bladder (Fig. 1B), similar to previous findings (Akagi et al., 2003). Treatment with BHA resulted in hyperkeratosis/parakeratosis and hyperplasia of stratified epithelia in the forestomach (Fig. 1C), similar to previous findings (Hirose et al., 1987). Treatment with CC resulted in pyloric gland hyperplasia of the glandular stomach (Fig. 1D), similar to previous findings (Hirose et al., 1999). Treatment with PhIP or CDCA did not induce any specific changes in the colon. CL as a non-carcinogenic control did not induce any changes in the epithelia of thyroid gland follicles, urinary bladder, forestomach, glandular stomach or colon. Untreated controls and carcinogens targeting other organs did not show histopathological alterations in each organ.

3.2. Immunohistochemical cellular distribution in the thyroid

In the thyroid, SDM induced a significant increase in Ki-67$^+$, p21^{Cip1+}, nuclear Cdc2$^+$ or p-Histone H3$^+$ follicular cells compared with the untreated controls, CL, BHA, CC or PhIP group (Fig. 2A–D). In contrast, BHA, CC and PhIP induced a significant decrease in Ki-67$^+$ cells compared with the untreated controls. On the other hand, CC induced a significant decrease in nuclear Cdc2$^+$ cells compared with the untreated controls. BHA induced a significant decrease in p-Histone H3$^+$ cells compared with the untreated controls. With regard to Aurora B, while SDM induced a tendency to increase in positive cells compared with the untreated controls, SDM induced a significant increase compared with CL, BHA, CC or PhIP group (Fig. 2E). With regard to HP1α, SDM did not induce a significant increase in positive cells (Fig. 2F). In comparison with the SDM group, BHA induced a significant decrease in HP1α$^+$ cells.

3.3. Immunohistochemical cellular distribution in the urinary bladder

In the urinary bladder, PEITC induced a significant increase in Ki-67$^+$, nuclear Cdc2$^+$ and p-Histone H3$^+$ cells compared with the untreated controls, CL, BHA, CC or PhIP group (Fig. 3A, C and D). With regard to p21^{Cip1}, BHA induced a significant increase in positive cells compared with the PEITC group (Fig. 3B). With regard to Aurora B, PEITC induced a significant increase in positive cells compared with the untreated controls, CL, CC or PhIP group (Fig. 3E). PEITC did not induce a significant increase in HP1α$^+$ cells (Fig. 3F).

3.4. Immunohistochemical cellular distribution in the forestomach

In the forestomach, BHA induced a significant increase in the vertical length of immunoreactive cellular distribution of Ki-67, Aurora B and HP1α from the basement membrane compared with the untreated controls, CL, CC or PhIP group (Fig. 4A, E and F). BHA also induced a significant increase in the number of nuclear Cdc2$^+$ and p-Histone H3$^+$ cells compared with the untreated controls, CL, CC or PhIP group (Fig. 4C and D). BHA did not induce a significant increase in the number of p21^{Cip1+} cells (Fig. 4B).

3.5. Immunohistochemical cellular distribution in the glandular stomach

In the glandular stomach, CC induced a significant increase in Ki-67$^+$, p21^{Cip1+}, nuclear Cdc2$^+$, *p-Histone H3$^+$ and* Aurora B$^+$ cells compared with the untreated controls, CL, BHA or PhIP group (Fig. 5A–E). However, PhIP induced a significant increase in p21^{Cip1+} cells compared with the untreated controls. CL also induced a significant increase in Aurora B$^+$ cells compared with the untreated controls. With regard to HP1α, CC did not induce a significant increase in positive cells compared with the untreated controls, whereas BHA induced a significant increase (Fig. 5F).

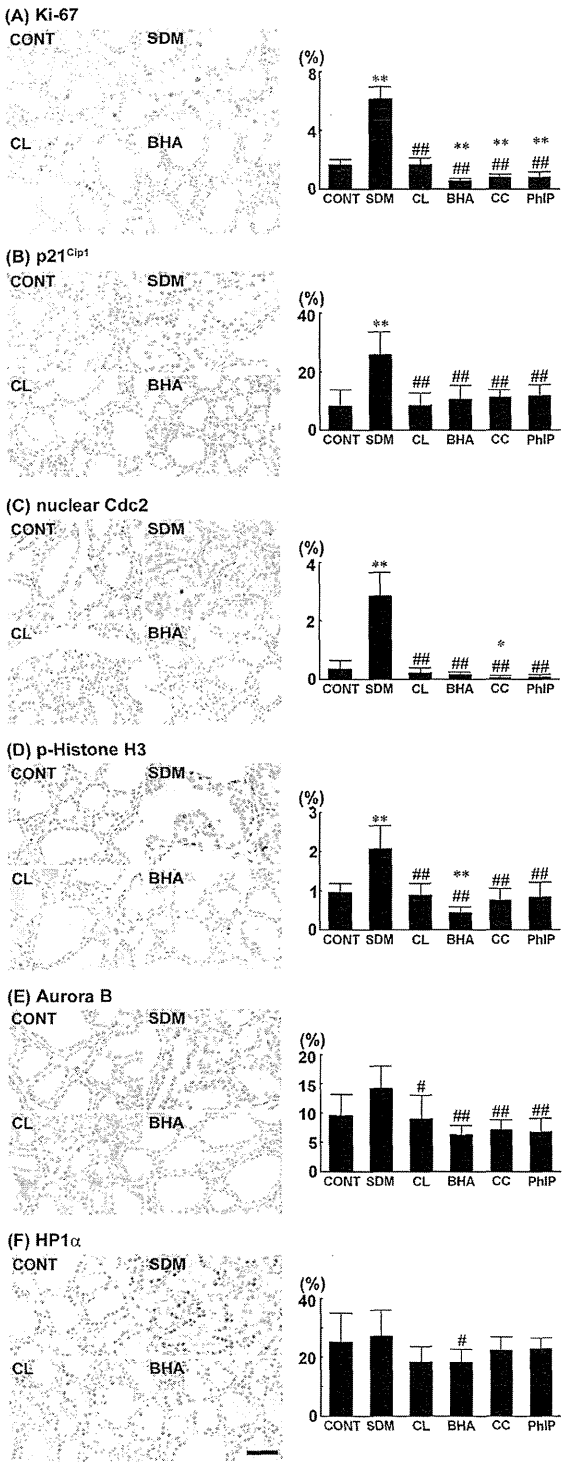

Fig. 2. Distribution of Ki-67$^+$, p21^{Cip1+}, nuclear Cdc2$^+$, p-Histone H3$^+$, Aurora B$^+$ and HP1α$^+$ cells in the thyroid. Photomicrographs show Ki-67$^+$, p21^{Cip1+}, nuclear Cdc2$^+$, p-Histone H3$^+$, Aurora B$^+$ and HP1α$^+$ cells in untreated controls and animals treated with SDM, CL or BHA. The graphs show positive cell ratios (%) of epithelial cells per total cells counted in each target organ using 10 animals per group. Values represent mean + SD. (A) Ki-67, (B) p21^{Cip1}, (C) nuclear Cdc2, (D) p-Histone H3, (E) Aurora B and (F) HP1α. Bar = 50 μm. $^{*,**}P < 0.0056$, 0.0011 vs. untreated controls (Student's *t*-test with Bonferroni correction). $^{\#,\#\#}P < 0.0056$, 0.0011 vs. SDM (Student's *t*-test with Bonferroni correction).

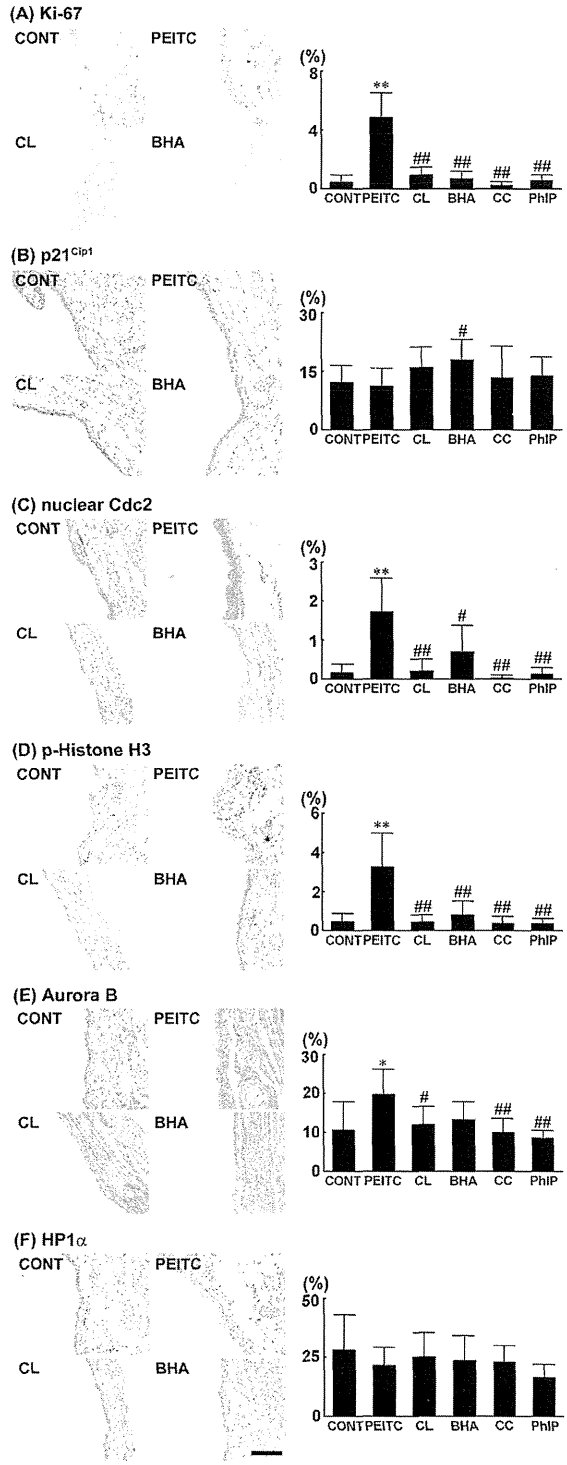

Fig. 3. Distribution of Ki-67$^+$, p21^{Cip1+}, nuclear Cdc2$^+$, p-Histone H3$^+$, Aurora B$^+$ and HP1α$^+$ cells in the urinary bladder. Photomicrographs show Ki-67$^+$, p21^{Cip1+}, nuclear Cdc2$^+$, p-Histone H3$^+$, Aurora B$^+$ and HP1α$^+$ cells in untreated controls and animals treated with PEITC, CL or BHA. The graphs show positive cell ratios (%) of epithelial cells per total cells counted in each target organ using 10 animals per group. Values represent mean + SD. (A) Ki-67, (B) p21^{Cip1}, (C) nuclear Cdc2, (D) p-Histone H3, (E) Aurora B and (F) HP1α. Bar = 100 μm. $^{*,**}P < 0.0056$, 0.0011 vs. untreated controls (Student's *t*-test with Bonferroni correction). $^{\#,\#\#}P < 0.0056$, 0.0011 vs. PEITC (Student's *t*-test with Bonferroni correction).

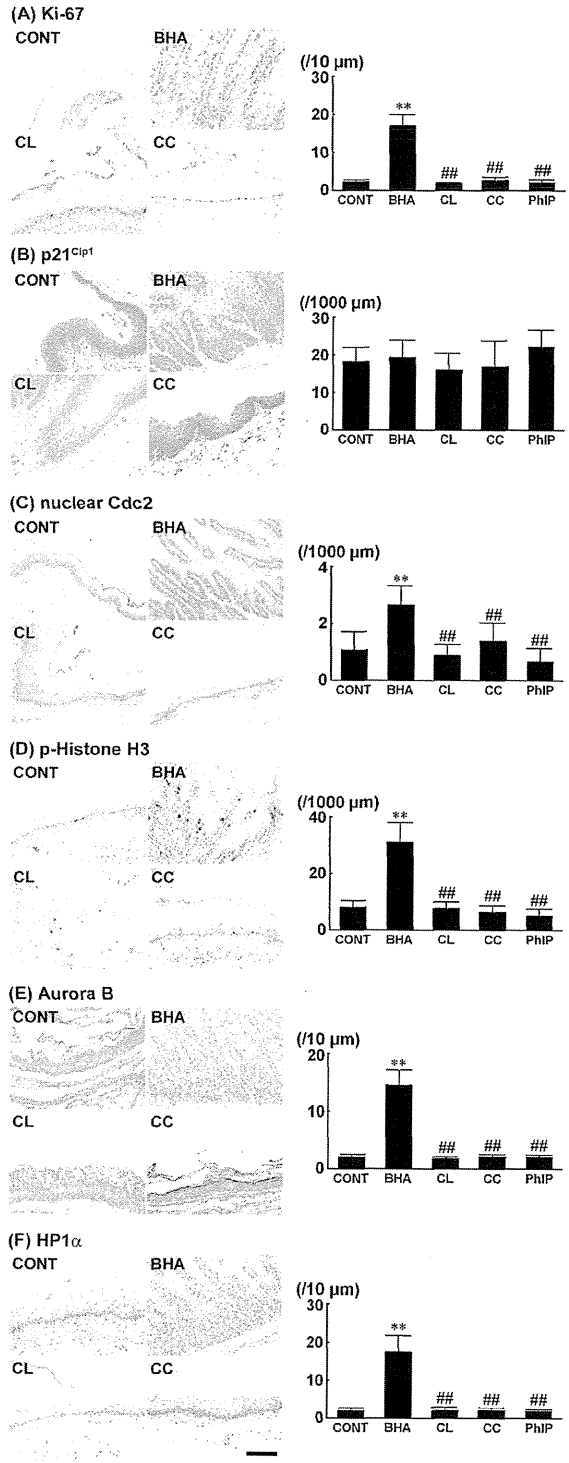

Fig. 4. Distribution of Ki-67$^+$, p21^{Cip1+}, nuclear Cdc2$^+$, p-Histone H3$^+$, Aurora B$^+$ and HP1α$^+$ cells in the forestomach. Photomicrographs show Ki-67$^+$, p21^{Cip1+}, nuclear Cdc2$^+$, p-Histone H3$^+$, Aurora B$^+$ and HP1α$^+$ cells in untreated controls and animals treated with BHA, CL or CC. (A), (E) and (F) show vertical length of positive cell distribution from the basement membrane per unit area using 10 animals per group. (B), (C) and (D) show mean number of positive cells per unit horizontal length (1000 μm). Values represent mean + SD. (A) Ki-67, (B) p21^{Cip1}, (C) nuclear Cdc2, (D) p-Histone H3, (E) Aurora B and (F) HP1α. Bar = 100 μm. $^{**}P < 0.0014$ vs. untreated controls (Student's *t*-test with Bonferroni correction). $^{\#\#}P < 0.0014$ vs. BHA (Student's *t*-test with Bonferroni correction).

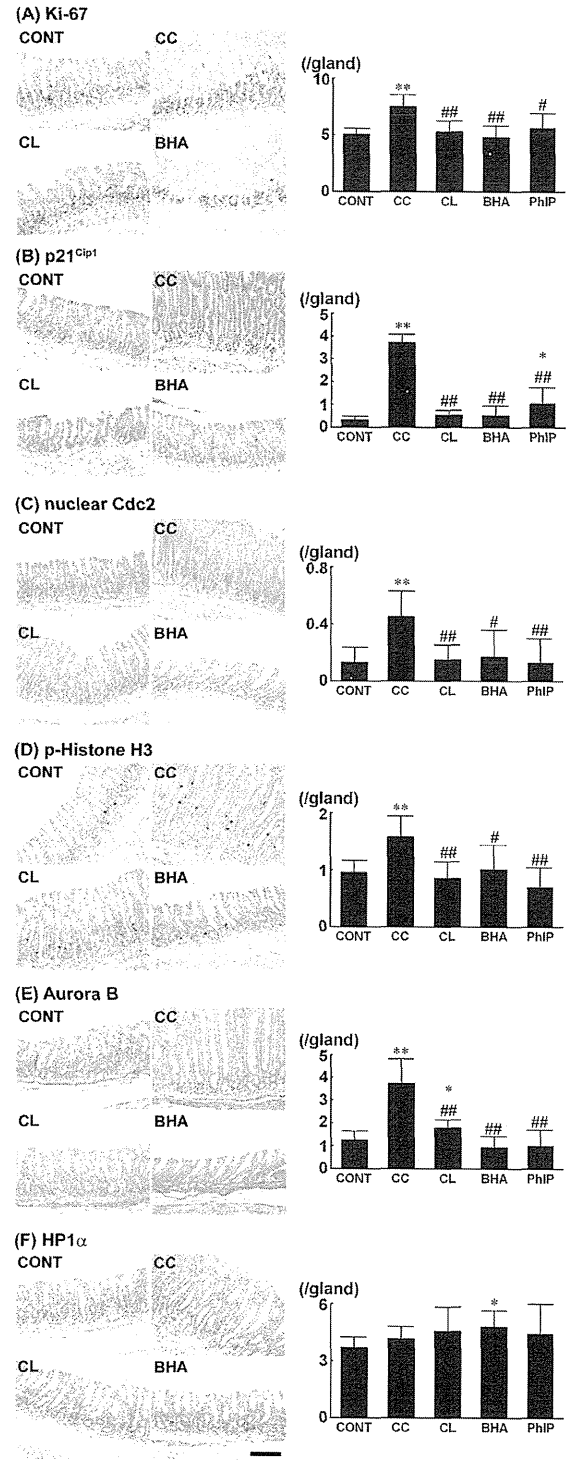

Fig. 5. Distribution of Ki-67$^+$, p21^{Cip1+}, nuclear Cdc2$^+$, p-Histone H3$^+$, Aurora B$^+$ and HP1α$^+$ cells in the glandular stomach. Photomicrographs show Ki-67$^+$, p21^{Cip1+}, nuclear Cdc2$^+$, p-Histone H3$^+$, Aurora B$^+$ and HP1α$^+$ cells in untreated controls and animals treated with CC, CL or BHA. The graphs show mean number of positive cells per gland using 10 animals per group. Values represent mean + SD. (A) Ki-67, (B) p21^{Cip1}, (C) nuclear Cdc2, (D) p-Histone H3, (E) Aurora B and (F) HP1α. Bar = 100 μm. $^{*,**}P < 0.0071, 0.0014$ vs. untreated controls (Student's *t*-test with Bonferroni correction). $^{\#,\#\#}P < 0.0071$, 0.0014 vs. CC (Student's *t*-test with Bonferroni correction).